

## The influence of textural and chemical properties of palm kernel shell activated carbon on the adsorption capacity and desorption efficiency of $\beta$ -carotene in a model system

<sup>1</sup>Ulfah, M., <sup>2\*</sup>Raharjo, S., <sup>2</sup>Hastuti, P. and <sup>2</sup>Darmadji, P.

<sup>1</sup>Department of Agricultural Technology, Institute of Agriculture STIPER, Jl. Nangka II, Maguwoharjo, Depok, Sleman, Yogyakarta, Indonesia, 55282.

<sup>2</sup>Department of Food and Agricultural Product Technology, Faculty of Agricultural Technology, Gadjah Mada University. Jl. Flora No. 1, Bulaksumur, Yogyakarta, Indonesia, 55281.

### Article history

Received: 30 November, 2016  
 Received in revised form:  
 4 May, 2017  
 Accepted: 21 September, 2018

### Abstract

The objectives of the present work were to characterise the textural and chemical properties of palm kernel shell activated carbon (PKSAC) prepared by chemical activation using phosphoric acid and its influence on the adsorption capacity and desorption efficiency of  $\beta$ -carotene in a model system. The PKSAC was prepared by impregnation of the precursor in phosphoric acid solution at ratios of 2 and 3 mL/g, and carbonisation at 500°C for 30, 45, 60 and 75 min. The results showed that the yield of all PKSAC was not significantly different. The PKSAC under impregnation ratio of 3 mL/g had higher surface area, total pore volume, mesopore and micropore volume than those at 2 mL/g. This resulted in the increase in  $\beta$ -carotene adsorption capacity by PKSAC at 3 mL/g. The textural properties of PKSAC and adsorption capacity under different carbonisation times were not significantly different. The PKSAC under impregnation ratio of 2 mL/g and carbonisation for 60 min (AC260) yielded the lowest non-polar surface functional group, whereas AC230 the highest. Non-polar surface functional groups might have increased the adsorption capacity but decreased the desorption efficiency, which was contrary with the polar functional group. AC260 also yielded the lowest adsorption capacity of  $\beta$ -carotene onto the PKSAC in a model system but yielded the highest desorption efficiency. .

© All Rights Reserved

### Keywords

Palm kernel shell activated carbon  
 $\beta$ -carotene  
 Adsorption capacity  
 Desorption efficiency

### Introduction

Palm kernel shells are often used as fuel source for boilers to generate bio-electricity and steam in the palm oil mills (Boateng and Lee, 2013). Common palm kernel shells contain high carbon (50.01%) (Mak *et al.*, 2009; Fuadi *et al.*, 2012), whereas palm kernel shells from the Tenera variety had a carbon content of 44.74%, ash content of 1.12%, total N content of 0.07%, and moisture content of 5.42% (Ulfah *et al.*, 2016). Therefore, palm kernel shells have the potential as a precursor of activated carbon.

A porous activated carbon can be made either by physical or chemical activation. Physical activation needs a temperature of up to 1000°C, whereas chemical activation temperature is within the range of 400-600°C (Hadoun *et al.*, 2013). Chemical activation using phosphoric acid ( $H_3PO_4$ ) has several advantages such as ease of carbonisation, low activation temperature, does not require  $N_2$  supply,

maximum adsorption capacity, bulk density and yield of product (Rahman *et al.*, 2012). The  $H_3PO_4$  acts as a catalyst to increase the breakdown of lignocellulosic matrix bonding and to enhance hydrolysis, condensation, dehydration and crosslinking reactions between  $H_3PO_4$  and constituent biopolymers contained in the biomass. These conditions can act as a template for the volume occupied by the acid from biomass activated to coincide with the pore volume of the activated carbon produced (Chowdhury *et al.*, 2013). Chemical activation with  $H_3PO_4$  to produce activated carbon from palm kernel shells has been studied by several researchers (Lim *et al.*, 2010; Allwar, 2012; Rahman *et al.*, 2012).

Adsorption is influenced by surface area of adsorbent, physical and chemical characteristics of the adsorbent, pH, and temperature (Çeçen and Aktaş, 2012). Crude palm oil (CPO) contains carotenoids as much as 630-700 ppm, mainly as  $\beta$ -carotene (Zeb and Mahmood, 2004), which is very useful in the

\*Corresponding author.  
 Email: [sraharjo@ugm.ac.id](mailto:sraharjo@ugm.ac.id)

field of food and health (Goeffrey, 2000; Min and Boff, 2002; Khachik, 2006; Zeb, 2011; Ariviani *et al.*, 2015).  $\beta$ -Carotene is a non-polar molecule with a length of 3.8 nm and height of 0.5 nm (Baró *et al.*, 2003). In physical refining, most of the  $\beta$ -carotene (up to 98%) was lost due to the bleaching and heating processes (Silva *et al.*, 2013). Therefore, it would be beneficial to recover  $\beta$ -carotene prior to physical refining, by adsorption and desorption methods using activated carbon.

Therefore, the present work was aimed to characterise palm kernel shell activated carbon prepared by chemical activation using  $H_3PO_4$  and its influence on the adsorption capacity and desorption efficiency of  $\beta$ -carotene in a model system.

## Materials and methods

### Materials

Palm kernel shell of Tenera variety was obtained from PT Smart Tbk. Indonesia. Orthophosphoric acid 85%, isopropyl alcohol, tetrahydrofuran and n-hexane were purchased from Merck, Germany.  $\beta$ -Carotene was purchased from Sigma-Aldrich (USA) and high purity nitrogen gas from Samator, Indonesia.

### Instrumentation

A Multi-Purpose Mill Model SNF-6-180 and the US sieve size 0.373-0.841 mm were used to obtain the uniform size of palm kernel shell particles. Oven (Memmert, Germany) and furnace (Thermolyne, USA) were used for carbonisation. The porosity of activated carbon was analysed by Quantacrome NovaWin2-NOVA Instrument. The microstructure of activated carbon was evaluated using SEM-EDS (JEOL JSM-6510LA). The surface functional groups of activated carbon were analysed by FTIR (Horizon MB 3000). An adsorption-desorption batch reactor equipped with a vacuum outlet,  $N_2$  gas inlet and stirring hot plate (Thermo Scientific CimarecTM, USA) was used. A centrifuge (Hettich EBA Zentrifugen 20, Germany) was used to separate the filtrate from activated carbon after the adsorption-desorption process. The concentration of  $\beta$ -carotene was analysed by UV-Vis Spectrophotometer (Shimadzu Uvmini 1240, Japan).

### Preparation of palm kernel shells activated carbon

Palm kernel shells were washed to remove dirt and fibre, and then boiled to remove residual oil. The cleaned shells were dried at 60°C in a cabinet dryer for 3 d, crushed, and sieved to obtain particle size within a range of 0.373-0.841 mm.

The preparation of palm kernel shells activated

carbon (PKSAC) was performed according to the method described by Lim *et al.* (2010) with slight modification. Briefly, palm kernel shell particles (60 g) were mixed with 65% phosphoric acid based on impregnation ratio at 2 and 3 mL/g, and soaked for 24 h at ambient temperature. Excess of phosphoric acid was drained with stainless steel filter and evaporated in the oven at 100-105°C for 4 h. The soaked palm kernel shells were semi-carbonised in the oven at 170°C for 1 h. The semi-carbonised materials were packed into 50 mL porcelain crucible up to 2/3 of volume, then activated in a muffle furnace at 500°C for 30, 45, 60 and 75 min with a heating rate of  $16.3 \pm 1.9^\circ\text{C}/\text{min}$ . For each activation process, the muffle furnace was filled with six properly labelled crucibles for the same carbonisation time. The activated materials were neutralised using hot distilled water so that the pH of 5 to 6 was reached. The neutralised PKSAC was dried in an oven around 80-90°C overnight, followed by drying at 110°C for 4 h, so that granular activated carbon was obtained.

The particles size of PKSAC was reduced to less than 0.419 mm to increase external surface area without changing the inside pore structure of the activated carbon (Lu *et al.*, 2015). From this preparation, powdered PKSAC which consisted of AC230 (2 mL/g for 30 min), AC245 (2 mL/g for 45 min), AC260 (2 mL/g for 60 min), AC275 (2 mL/g for 75 min), AC330 (3 mL/g for 30 min), AC345 (3 mL/g for 45 min), AC360 (3 mL/g for 60 min) and AC375 (3 mL/g for 75 min) treatments were obtained.

### Yield of activated carbon

The yields of activated carbon were calculated using Equation 1:

$$\text{Yield (\%)} = \frac{\text{Massa of activated Carbon(g)}}{\text{Massa of precursor(g)}} \times 100$$

(Equation 1)

### Textural characteristics

The textural characteristics of PKSAC were analysed by  $N_2$  adsorption-desorption at 77.3 K and relative pressure (P/Po) from 0,005 to 0.999 using a surface area analyser (Quantacrome NovaWin2-NOVA Instrument). The textural characteristics of PKSAC including surface area and total pore volume were determined by Brunauer-Emmet-Teller (BET) method, the mesopore size distribution was determined by Barret-Joyner-Halenda (BJH) method, the micropore size distribution was determined by Horvarth-Kawazoe (HK) method, and the micropore volume was determined by Saito-Foley (SF) method.

### Elemental matters

The elemental composition of PKSAC was determined using scanning electron microscopy (SEM-JEOL JSM-6510LA) equipped with energy dispersive spectrometer (EDS). The EDS spectra showing elemental composition were obtained by scanning the surfaces of the samples. The surface distributions were collected from SEM pictures using different magnifications.

### Surface functional groups

The surface functional groups of PKSAC was estimated based on the transmittance spectrum of the organic components produced using Fourier Transform Infrared Spectrometer (Horizon MB 3000). The spectra were recorded from 4000-500  $\text{cm}^{-1}$ . By comparison to the standard frequency patterns, various characteristic chemical bonds were determined from which certain surface functional groups were derived.

### Adsorption of $\beta$ -carotene onto PKSAC in a model system

The adsorption reactor was made from a 125 mL conical flask equipped with a vacuum outlet,  $\text{N}_2$  gas inlet, thermometer and hot plate stirrer, and was performed according to Muhammad *et al.* (2010) with slight modification. Briefly, 500 mg/L  $\beta$ -carotene was dissolved in isopropyl alcohol, placed into a conical flask and then activated carbon was added at 1.5%. The adsorption process was conducted at 50°C. Following equilibration, the filtrate was separated from each activated carbon by centrifugation at 4,500 rpm for 10 min. The concentration of  $\beta$ -carotene was analysed using PORIM test (Fauzi and Sarmidi, 2010). The adsorption capacity at equilibrium can be calculated using Equation 2 (Muhammad *et al.*, 2010):

$$q_e = \frac{V(C_o - C_e)}{m} \quad (\text{Equation 2})$$

where  $q_e$  was adsorption capacity at equilibrium phase (mg/g),  $C_o$  was the initial concentration in the liquid phase (mg/L),  $C_e$  was the liquid phase concentration at the equilibrium (mg/L),  $V$  was the volume of liquid (L), and  $m$  was the mass of activated carbon (g).

### Desorption of $\beta$ -carotene

The desorption of  $\beta$ -carotene was carried out at 40°C for 5 min using tetrahydrofuran. The desorption efficiency was calculated based on Muhammad *et al.* (2011) using Equations 3 and 4:

$$Eff(\%) = \frac{q_e - q_i}{q_e} \times 100 \quad (\text{Equation 3})$$

$$q_i = q_e - \left( \frac{V \cdot C_d}{m} \right) \quad (\text{Equation 4})$$

where  $q_i$  was the concentration of  $\beta$ -carotene in activated carbon after desorption (mg/g),  $C_d$  was the concentration of  $\beta$ -carotene in liquid phase after desorption (mg/L), and  $Eff$  was the desorption efficiency (%).

### Experimental design

The present work was conducted using a randomised complete block design with two factors namely the impregnation ratios (2 and 3 mL/g) and carbonisation times (30, 45, 60 and 75 min). The data were subjected to Analysis of Variance (ANOVA) and the significance of the difference among means was determined by Duncan's multiple range test ( $p < 0.05$ ).

## Results and discussion

### Yields of activated carbon

The yields of PKSAC were in the range of 47.33 - 48.17% and not influenced by the ratio of impregnation or the carbonisation time (Table 1). These yields are consistent with the results of previous research. Bedmohata *et al.* (2015) showed that activated carbon produced with the ratio of  $\text{H}_3\text{PO}_4$  and lignin with a range of 0.5:1 to 2:1 mL/g at 600°C for 1 h yielded 44.38-58.42%. Mi *et al.* (2015) produced activated carbon with a yield of 48-50% by impregnation using 70%  $\text{H}_3\text{PO}_4$  for 12 h and carbonisation temperature of 550°C for 20-65 min. While Abechi *et al.* (2013) produced activated carbon with a yield range of 43.38-46.33% at carbonisation temperature of 800°C for 15-45 min. According to Lim *et al.* (2010), the impregnation ratio did not change the reaction kinetics between carbonaceous materials and  $\text{H}_3\text{PO}_4$ . During the thermal decomposition of lignocellulosic materials, the diffusion of  $\text{H}_3\text{PO}_4$  into the material would limit the formation of tar through the formation of crosslinks and inhibit the shrinkage of material particles, because the  $\text{H}_3\text{PO}_4$  had occupied a considerable volume. The  $\text{H}_3\text{PO}_4$  formed a bonding layer as a  $\text{H}_3\text{PO}_4$  or polyphosphate ester that would protect the inner pores structure of the adsorbent and prevent over-burning. The evolution of chemical processes due to activation using  $\text{H}_3\text{PO}_4$  starts at lower temperatures which could result in high yield of activated carbon.

Table 1. Yield and textural characteristics of palm kernel shell activated carbons.

| Impregnation ratio (ml/g)   | Yield (%) | S <sub>BET</sub> (m <sup>2</sup> /g) | V <sub>t</sub> (cc/g) | S <sub>meso</sub> (m <sup>2</sup> /g) | V <sub>meso</sub> (cc/g) | R <sub>meso</sub> (Å) | V <sub>micro</sub> (cc/g) |
|-----------------------------|-----------|--------------------------------------|-----------------------|---------------------------------------|--------------------------|-----------------------|---------------------------|
| 2                           | 47.96     | 1383.98 <sup>a</sup>                 | 0.80 <sup>a</sup>     | 137.63 <sup>a</sup>                   | 0.16 <sup>a</sup>        | 15.32                 | 0.58 <sup>a</sup>         |
| 3                           | 47.87     | 1459.06 <sup>b</sup>                 | 0.85 <sup>b</sup>     | 154.12 <sup>b</sup>                   | 0.18 <sup>b</sup>        | 15.30                 | 0.61 <sup>b</sup>         |
| Time of carbonisation (min) | Yield (%) | S <sub>BET</sub> (m <sup>2</sup> /g) | V <sub>t</sub> (cc/g) | S <sub>meso</sub> (m <sup>2</sup> /g) | V <sub>meso</sub> (cc/g) | R <sub>meso</sub> (Å) | V <sub>micro</sub> (cc/g) |
| 30                          | 48.17     | 1426.10                              | 0.83                  | 146.72                                | 0.17                     | 15.31                 | 0.60                      |
| 45                          | 48.11     | 1437.88                              | 0.83                  | 141.06                                | 0.16                     | 15.31                 | 0.60                      |
| 60                          | 48.04     | 1407.39                              | 0.81                  | 141.98                                | 0.16                     | 15.34                 | 0.59                      |
| 75                          | 47.33     | 1414.72                              | 0.82                  | 153.72                                | 0.18                     | 15.28                 | 0.59                      |

Means not sharing a common letter in a column are significantly different at  $p < 0.05$ . S<sub>BET</sub> : surface area; V<sub>t</sub> : total pore volume; S<sub>meso</sub> : mesopore surface area; R<sub>meso</sub> : mesopore radius, V<sub>micro</sub> : micropore volume

### Textural properties of palm kernel shell activated carbon

Textural properties of PKSAC are summarised in Table 1. It can be seen that impregnation ratio of 2 mL/g had lower BET surface area, total pore volume, mesopore surface area, mesopore volume, and micropore volume than that of 3 mL/g. According to Lim *et al.* (2010), the porosity of the activated carbon increased with increasing impregnation ratio. Phosphoric acid would minimise the formation of tar and other liquids that could clog pores and inhibit the development of the activated carbon pore structure. The hydrated H<sub>3</sub>PO<sub>4</sub> during activation remained as the salt of H<sub>3</sub>PO<sub>4</sub> inside the porous structure of activated carbon, thus occupying a sufficiently large volume. After the H<sub>3</sub>PO<sub>4</sub> salts that formed during activation were removed from the activated carbon by washing with water, the total pore volume would then increase.

The resulting PKSAC had textural properties which were not significantly different, with a large surface area and high pore volume. This showed that carbonisation for 30-75 min at 500°C with a heating rate of  $16.3 \pm 1.9^\circ\text{C}/\text{min}$  could produce porous activated carbon.

According to Chowdhury *et al.* (2013), H<sub>3</sub>PO<sub>4</sub> can act as a catalyst to breaker the bond of the lignocellulosic matrix and encourage hydrolysis, condensation and dehydration. This encouraged the cross-linking reactions between H<sub>3</sub>PO<sub>4</sub> and the biopolymer constituents present in the biomass. This condition could act as a template because the volume occupied by acid from the activated biomass coincided with the pore volume of the activated carbon produced. The increase in total pore volume would therefore increase the surface area of activated carbon.

### Elemental composition of palm kernel shell activated carbon

The elemental composition of PKSAC observed in the present work, which included carbon (C), oxygen (O), nitrogen (N), sulphur (S) and phosphorus (P), are shown in Table 2. Carbon (62.22-67.55%) was the highest in AC260. Oxygen (17.61-19.54%) was not significantly different between each activated carbon types. Nitrogen (12.78-18.43%) was the lowest in AC260. Sulphur (0.06-0.36%) was also not significantly different between each activated carbon types. Phosphorus (0.77-1.70%) was the in AC260.

Table 2. The elemental composition of palm kernel shell activated carbons under different impregnation ratios and times of carbonisation.

| Activated carbon types | Element types (%)         |              |                           |                          |                          |
|------------------------|---------------------------|--------------|---------------------------|--------------------------|--------------------------|
|                        | C                         | O            | N                         | S                        | P                        |
| AC230                  | 62.34 ± 0.60 <sup>b</sup> | 18.27 ± 0.11 | 18.43 ± 0.52 <sup>a</sup> | 0.12 ± 0.06 <sup>b</sup> | 0.79 ± 0.13 <sup>c</sup> |
| AC245                  | 62.54 ± 0.86 <sup>b</sup> | 18.69 ± 0.82 | 17.92 ± 0.02 <sup>b</sup> | 0.09 ± 0.04 <sup>c</sup> | 0.77 ± 0.03 <sup>c</sup> |
| AC260                  | 67.55 ± 0.55 <sup>a</sup> | 17.61 ± 0.42 | 12.78 ± 0.07 <sup>d</sup> | 0.36 ± 0.04 <sup>a</sup> | 1.70 ± 0.10 <sup>a</sup> |
| AC275                  | 63.05 ± 0.14 <sup>b</sup> | 19.54 ± 0.22 | 16.52 ± 0.41 <sup>c</sup> | 0.06 ± 0.01 <sup>c</sup> | 0.84 ± 0.03 <sup>c</sup> |
| AC330                  | 62.87 ± 1.04 <sup>b</sup> | 18.76 ± 0.52 | 17.59 ± 0.50 <sup>b</sup> | 0.08 ± 0.04 <sup>c</sup> | 0.72 ± 0.01 <sup>c</sup> |
| AC345                  | 62.42 ± 0.54 <sup>b</sup> | 18.90 ± 0.81 | 17.88 ± 0.37 <sup>b</sup> | 0.06 ± 0.00 <sup>c</sup> | 0.76 ± 0.11 <sup>c</sup> |
| AC360                  | 62.41 ± 0.01 <sup>b</sup> | 19.24 ± 0.04 | 17.44 ± 0.06 <sup>b</sup> | 0.07 ± 0.01 <sup>c</sup> | 0.85 ± 0.04 <sup>b</sup> |
| AC375                  | 62.22 ± 0.01 <sup>b</sup> | 19.54 ± 0.61 | 17.42 ± 0.59 <sup>b</sup> | 0.07 ± 0.01 <sup>c</sup> | 0.82 ± 0.05 <sup>c</sup> |

Means not sharing a common letter in a column are significantly different at  $p < 0.05$

Activated carbon of AC260 contained carbon, sulphur and phosphorus the highest. The high carbon content in activated carbon would support its ability to adsorb non-polar compounds such as  $\beta$ -carotene, but the sulphur and phosphorus were likely to inhibit its ability to adsorb of  $\beta$ -carotene.

*Surface functional groups of palm kernel shell activated carbon*

The surface functional groups of PKSAC prepared at different conditions are summarised in Table 3, whereas the FTIR spectra for PKSAC are presented in Figure 1. Table 3 shows the alkyl mercaptan from S-H stretch (Lambert *et al.*, 1987) found only in AC360, and alcohol and phenol from H-bonded (Lambert *et al.*, 1987) in AC275. Phosphine from P-H (Lambert *et al.*, 1987), C-N stretch in secondary amine (Coates, 2000), C-N stretch in primary amine (Coates, 2000), C-O-C antisym stretch in aliphatic ether (Lambert *et al.*, 1987), C-H out-of-plane bend

in vinyl (Coates, 2000), C-H bend in alkyne (Coates, 2000) were found in all PKSACs. Isocyanates from N=C=O antisym stretch (Lambert *et al.*, 1987) was only found in AC360. Aromatic ring from C=C-C and C-N stretch in the primary amine (Coates, 2000) were found in all PKSACs except for AC260. The NO<sub>2</sub> antisym stretch in the aromatic nitro compound, organic sulphate group and C-O stretch in alcohol (Coates, 2000) were only found in AC260.

Activated carbon AC260 showed the most polar surface functional groups. These groups were not present in other activated carbon. All activated carbon except AC260 had FTIR spectra at wave number 2,704-3,094 m<sup>-1</sup> which showed the spectra of non-polar functional groups (Figure 1). The polarity of activated carbon surface will determine the  $\beta$ -carotene adsorption capacity. Non-polar surface functional groups will make it easy to adsorb  $\beta$ -carotene onto activated carbon, whereas polar surface functional groups will inhibit adsorption capacity of  $\beta$ -carotene.

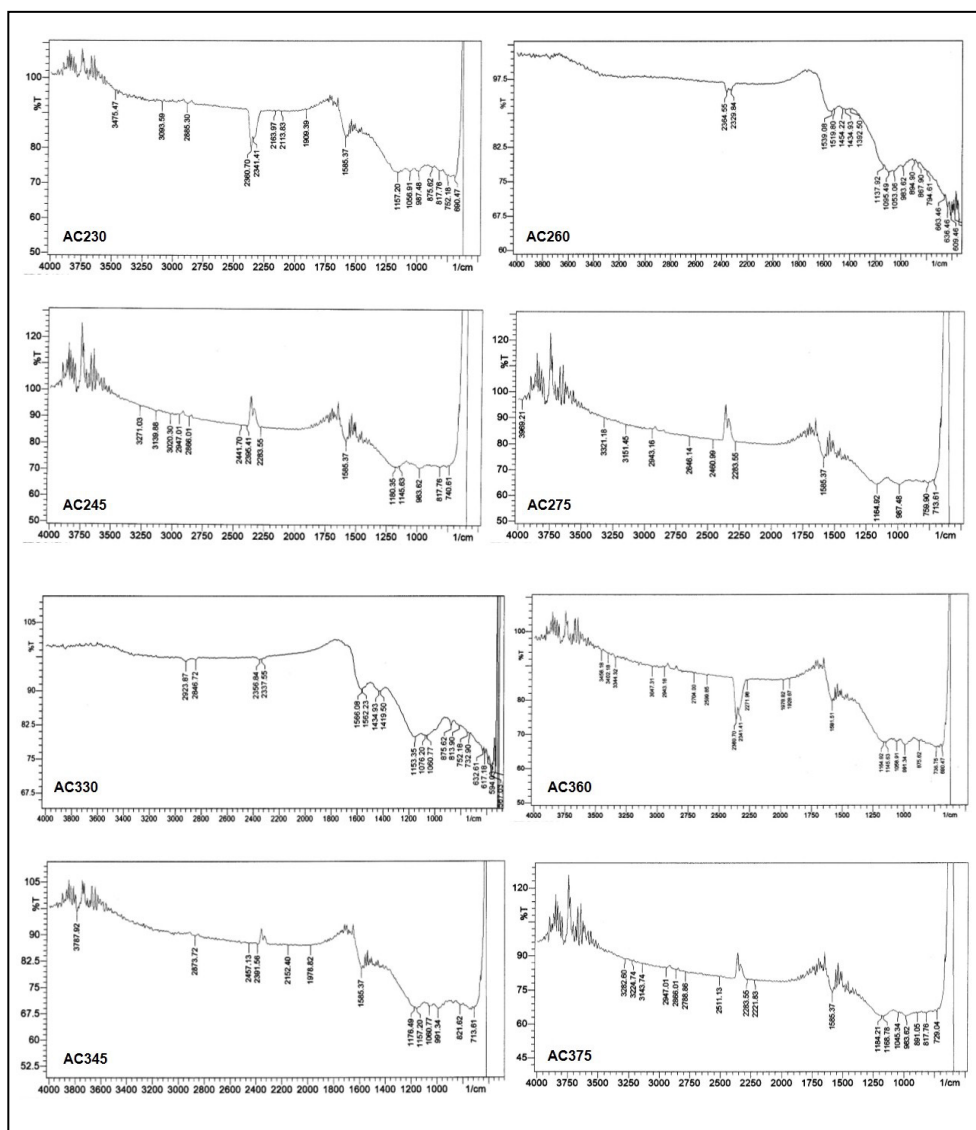


Figure 1. The FTIR spectra for palm kernel shell activated carbons.

Table 3. Surface functional groups composition of palm kernel shell activated carbons.

| Wave number of FTIR spectra (1/cm) | Contained in PKSAC                                     | Functional groups  | References                                  |
|------------------------------------|--|--|---|
| 3217-3283                          | AC230, AC245, AC275, AC360, AC375                      | OH stretch in hydroxy group; NH stretch in primary and secondary amine   | Lambert <i>et al.</i> (1987)                |
| 3020-3094                          | AC230, AC245, AC360                                    | =C-H stretch in aromatic   | Lambert <i>et al.</i> (1987)                |
| 2874-2947                          | AC245, AC275, AC345, AC360, AC375                      | CH asym/sym stretch in aliphatic compound                                | Lambert <i>et al.</i> (1987)                |
| 2866-2885                          | AC230, AC245, AC345, AC375                             | C-H stretch in methylene ; C-H asym/sym stretch in methyl                | Coates (2000)                               |
| 2704-2847                          | AC275, AC330, AC360, AC375                             | C-H stretch in aldehyde  | Lambert <i>et al.</i> (1987)                |
| 2461-2789                          | AC245, AC360, AC375                                    | H-bond-OH stretch in carboxylic acid                                     | Lambert <i>et al.</i> (1987)                |
| 2511-2646                          | AC275, AC360, AC375                                    | -NH stretch in amine hydrohalide   | Lambert <i>et al.</i> (1987)                |
| 2646-2560                          | AC275, AC360   | -OH stretch in phosphorus oxyacid  | Lambert <i>et al.</i> (1987)                |
| 2560                               | AC360  | S-H stretch in alkyl mercaptan   | Lambert <i>et al.</i> (1987)                |
| 2450                               | AC275  | H-bonded in alcohol and phenol   | Lambert <i>et al.</i> (1987)                |
| 2361-2604                          | AC230, AC260, AC275, AC345, AC360, AC375               | -NH stretch in amine   | Lambert <i>et al.</i> (1987)                |
| 2284-2392                          | AC230, AC245, AC260, AC275, AC330, AC345, AC360, AC375 | P-H in phosphine   | Lambert <i>et al.</i> (1987)                |
| 2272-2338                          | AC345, AC360   | N=N stretch in diazonium salt  | Lambert <i>et al.</i> (1987)                |
| 2272                               | AC360  | N=C=O antisym stretch in isocyanate                                      | Lambert <i>et al.</i> (1987)                |
| 2114-2222                          | AC230, AC345, AC375                                    | C≡C stretch in acetylenic  | Coates (2000)                               |
| 1880-1929                          | AC230, AC345, AC360                                    | “Combi” in aromatic combination bend                                     | Coates (2000)                               |
| 1582-1585                          | AC230, AC245, AC275, AC330, AC345, AC360, AC376        | C=C-C in aromatic ring; N-H bend in primary amine                        | Coates (2000)                               |
| 1540                               | AC260  | NO <sub>2</sub> antisym stretch in aromatic nitro compound               | Coates (2000)                               |
| 1435-1454                          | AC260, AC330   | C-H asym/sym bend in methyl  | Coates (2000)                               |
| 1393                               | AC260  | Organic sulphate   | Coates (2000)                               |
| 1138-1184                          | AC230, AC245, AC260, AC275, AC330, AC345, AC360, AC375 | C-N stretch in secondary amine; C-O-C antisym stretch in aliphatic ether | Lambert <i>et al.</i> (1987); Coates (2000) |
| 1095                               | AC260  | C-O stretch in alcohol   | Lambert <i>et al.</i> (1987)                |
| 1041-1076                          | AC230, AC260, AC275, AC330, AC345, AC360, AC375        | C-N stretch in primary amine   | Coates (2000)                               |
| 984-991                            | AC230, AC245, AC260, AC275, AC330, AC345, AC360, AC375 | C-H out-of-plane bend in vinyl   | Coates (2000)                               |
| 818-883                            | AC230, AC245, AC260, AC275, AC330, AC345, AC360, AC375 | C-H bend in alkyne   | Coates (2000)                               |
| 609-714                            | AC230, AC260, AC275, AC330, AC345, AC360               | O-H out-of-plane bend in alcohol   | Coates (2000)                               |
| 567-579                            | AC275, AC330   | C-I stretch in aliphatic iodo compounds                                  | Lambert <i>et al.</i> (1987)                |

*β-Carotene adsorption capacity*

Adsorption of  $\beta$ -carotene in a model system was using isopropyl alcohol (IPA) because IPA is less dissolving of  $\beta$ -carotene, but can dissolve the oil completely. IPA can dissolve the  $\beta$ -carotene at 40 mg/L (Craft, 1992), and had good solvency for crude palm oil and homogeneous at 50°C (Baharin *et al.*, 1998). The adsorption capacity of  $\beta$ -carotene onto PKSAC are shown in Table 4. The adsorption capacity of  $\beta$ -carotene onto PKSAC under impregnation ratio of 3 mL/g was significantly higher than that of at 2 mL/g. This might be caused by the increase in the surface area, total pore volume and mesopore surface area of activated carbon produced at impregnation ratio of 3 mL/g. The adsorption capacity of PKSAC under carbonisation at 500°C for 30-75 min were not significantly different. This was further supported by the textural properties of PKSAC which were not significantly different between different carbonisation times. The AC330 treatment had the highest adsorption capacity. The adsorption capacity of activated carbon, other than determined by its textural properties, according to Guo and Lua (2002), was also influenced by its surface chemistry that determined by types of surface functional groups. The AC330 treatment had higher surface area, total pore volume and mesopore volume than other PKSAC samples, thus supporting the adsorption of  $\beta$ -carotene. According to Lim *et al.* (2010), the increase of iodine adsorption capacity well reflects the increase in porosity of the activated carbon. The AC330 treatment also had higher non-polar functional groups than polar groups, which might have yielded the highest  $\beta$ -carotene adsorption capacity. The non-polar surface functional groups included C-H stretch in aldehyde, C=C-C in the aromatic ring, C-H asym/sym bend in methyl, C-O-C antisym stretch in the aliphatic ether, C-H out-of-plane bend vinyl and C-H bend in alkyne. Whereas the polar surface functional groups included N-H bend or C-N stretch in the primary amine, C-N stretch in secondary amine and O-H out-of-plane bend in alcohol.

On the contrary, the AC260 treatment had the lowest adsorption capacity since it had the lowest surface area, total pore volume and mesopore volume as compared to the other PKSAC samples. The low adsorption capacity of AC260 treatment might have been caused by polar surface functional groups which were higher than non-polar groups. The polar surface functional groups in AC260 included -NH stretch in the amine, P-H in phosphine, NO<sub>2</sub> antisym stretch in the aromatic nitro compound, an organic sulphate, C-N stretch in the secondary amine, C-O stretch in alcohol and O-H out-of-plane bend in alcohol.

Whereas the non-polar surface functional groups included C-H asym/sym bend in methyl, C-O-C antisym stretch in the aliphatic ether, C-H out-of-plane bend in vinyl and C-H bend in alkyne.

Table 4.  $\beta$ -Carotene adsorption capacity onto PKSAC and desorption efficiency.

| Impregnation ratio (mL/g)   | Adsorption capacity (mg/g) | Desorption efficiency (%) |
|-----------------------------|----------------------------|---------------------------|
| 2                           | 12.06 <sup>a</sup>         | 73.89 <sup>a</sup>        |
| 3                           | 12.54 <sup>b</sup>         | 60.25 <sup>b</sup>        |
| Time of carbonisation (min) | Adsorption capacity (mg/g) | Desorption efficiency (%) |
| 30                          | 12.78                      | 58.29                     |
| 45                          | 11.97                      | 74.53                     |
| 60                          | 11.96                      | 76.86                     |
| 75                          | 12.47                      | 58.61                     |

Means not sharing a common letter in a column are significantly different at  $p < 0.05$

*Desorption efficiency of β-carotene*

The desorption efficiency of  $\beta$ -carotene from the surface of the pores activated carbon was performed using tetrahydrofuran. According to Craft (1992), tetrahydrofuran can dissolve  $\beta$ -carotene as much as 10,000 mg/L higher than n-hexane. The  $\beta$ -carotene desorption efficiency of PKSAC is shown in Table 4. The desorption efficiency of  $\beta$ -carotene at a ratio of impregnation of 2 mL/g was higher than that at 3 mL/g. This might be due to the surface area of activated carbon at a ratio of impregnation of 3 mL/g which was greater than that at 2 mL/g.  $\beta$ -Carotene desorption efficiencies of PKSAC under carbonisation temperature of 500°C for 30-75 min were not significantly different. This was supported by the textural properties of PKSAC which were also not significantly different between different carbonisation times.

Greater activated carbon surface area could cause the adsorbent to bond with the surface of activated carbon, so the release of the adsorbent from the surface of the pores might be difficult which consequently leads to a lower desorption efficiency. According to Mohammad *et al.* (2011), the activation energy for diffusion of the adsorbent in the liquid and gas from the surface of microporous activated carbon will be greater than the mesopore or macropore. Intra-particle diffusion would be difficult if through narrow pores. Microporous activated carbon can trap on the adsorbent and make it difficult to diffuse from the pores of the adsorbent. Mohammad *et al.* (2011) also stated that the cylindrical geometry of the  $\beta$ -carotene molecule could also be the reason for blocking the diffusion paths, thus affecting the efficiency desorption.

The desorption efficiency of the AC260 treatment was the highest, whereas AC330 the lowest. This is contrary with the adsorption capacity. The higher desorption efficiency of AC260 treatment might have been caused by the surface area, total pore volume and micropore volume were of AC330 which were lower than the other PKSAC samples. The desorption efficiency was also influenced by the surface functional groups found on the activated carbon pore. The increase in non-polar surface functional groups could have also caused the low desorption efficiency. This might be due to the fact that the activated carbon surface had strong affinity with  $\beta$ -carotene.

## Conclusion

Adsorption and desorption of  $\beta$ -carotene in a model system were influenced by the textural and chemical properties of powdered palm kernel shell activated carbon. The increasing porosity and the amount of non-polar surface functional groups of the activated carbon increased  $\beta$ -carotene adsorption capacity but decreased desorption efficiency. This was evident at impregnation ratio of 3 mL/g, with adsorption capacity and desorption efficiency of 12.54 mg/g and 60.25%, respectively. When the activated carbon were carbonised for 30 min, the adsorption capacity and desorption efficiency was 12.78 mg/g and 58.29%, respectively. The activated carbon prepared with impregnation ratio of 2 mL/g had the lowest  $\beta$ -carotene adsorption capacity of 12.06 mg/g, but highest desorption efficiency of 73.89%. When activated carbon was carbonised for 60 min, the adsorption capacity and desorption efficiency was 11.96 mg/g and 75.86%, respectively.

## Acknowledgement

The present work was financially supported by Research Grant 2015-2017 provided by the Universitas Gadjah Mada and the Ministry of Research, Technology, and Higher Education, Republic of Indonesia.

## References

- Abechi, S. E., Gimba, C. E., Uzairu, A. and Dallatu, Y. A. 2013. Preparation and characterization of activated carbon from palm kernel shell by chemical activation. *Research Journal of Chemical Sciences* 3(7): 54-61.
- Allwar, A. 2012. Characteristics of micro- and mesoporous structure and surface chemistry of activated carbons produced by oil palm shell. *International Conference on Chemical, Ecology and Environmental Sciences Proceedings*, p. 138-141. Bangkok.
- Ariviani, S., Anggrahini, S., Naruki, S. and Raharjo, S. 2015. Characterization and chemical stability evaluation of  $\beta$ -carotene microemulsions prepared by spontaneous emulsification method using VCO and palm oil as oil phase. *International Food Research Journal* 22(6): 2432-2439.
- Baharin, B. S., Abdul Rahman, K., Abdul Karim, M. I., Oyaizu, T., Tanaka, K., Tanaka, Y. and Takagi, S. 1998. Separation of palm carotene from crude palm oil by adsorption chromatography with a synthetic polymer adsorbent. *Journal of the American Oil Chemists' Society* 75(3): 399-404.
- Baró, A. M., Hla, S. W. and Rieder, K. H. 2003. LT-STM study of self-organization of  $\beta$ -carotene molecular layers on Cu (111). *Chemical Physics* 369: 240-247.
- Bedmohata, M. A., Singh, S. P., Chaudhari, A. and Choudhary, M. D. 2015. Adsorption capacity of activated carbon prepared by chemical activation of lignin for the removal of methylene blue dye. *International Journal of Advanced Research in Chemical Science* 2(8): 1-13.
- Boateng, C. O. and Lee K. T. 2013. Sustainable utilization of oil palm wastes for bioactive phytochemicals for the benefit of the oil palm and nutraceutical industries. *Phytochemistry Reviews* 12: 173-190.
- Bouchemal, N., Belhachemi, M., Merzougui, Z. And Addoun, F. 2009. The effect of temperature and impregnation ratio on the active carbon porosity. *Desalination and Water Treatment* 10: 115-120.
- Çeçen, F. and Akaş, O. 2012. *Activated Carbon for Water and Wastewater Treatment*. Weinheim: Wiley-VHC.
- Coates, J. 2000. Interpretation of infrared spectra, a practical approach. In Meyers, R.A. (Ed.). *Encyclopedia of Analytical Chemistry*, p. 10815–10837. Chichester: John Wiley and Sons Ltd.
- Chowdhury, Z. Z., Hamid, S. B. A., Das, R., Hasan, M. R., Zain, S. M., Khalid, K. and Uddin, M. N. 2013. Preparation of carbonaceous adsorbents from lignocellulosic biomass and their use in removal of contaminants from aqueous solution. *BioResources* 8(4): 6523-6555.
- Craft, N. E. 1992. Relative solubility, and absorptivity of lutein and  $\beta$ -carotene in organic solvents. *Journal of Agricultural and Food Chemistry* 40: 431-434.
- Durán-Valle, C. J. 2012. *Techniques Employed in Physicochemical Characterization of Activated Carbons*. Retrieved from website: [www.intechopen.com](http://www.intechopen.com)
- Fuadi, N. A., Ibrahim, A. S. and Ismail, K. N. 2012. Review study for activated carbon from palm shell used for treatment of waste water. *Journal of Purity, Utility Reaction and Environmental* 1(5): 252-266.
- Geoffrey, H. W. 2000. European Patent No. EP 0 666 845 B1. Kirkland, Washington: US. European Patent Office
- Guo, J. and Lua, A. 2002. Textural and chemical characterizations of adsorbent prepared from palm shell by potassium hydroxide impregnation at different stages. *Journal of Colloid and Interface Science* 254: 227-233.

- Hadoun, H., Sadaoui, Z., Souami, N., Sahel, D. and Toumert, I. 2013. Characterization of mesoporous carbon prepared from date stems by  $H_3PO_4$  chemical activation. *Applied Surface Science* 280: 1-7.
- Khachik, F. 2006. U.S Patent No. 7, 119, 238 B2. Maryland, MD: U.S. Patent and Trademark Office
- Lambert, J. B., Shurvell, H. F. and Cooks, R. G. 1987. *Introduction to Organic Spectroscopy* 1st ed. New York: Macmillan Publication.
- Lim, W. C., Srinivasakannan, C. and Balasubramanian, N. 2010. Activation of palm shell by phosphoric acid impregnation for high yielding activated carbon. *Journal of Analytical and Applied Pyrolysis* 88: 181-186.
- Lu, C., Pan, L. and Zhuc, B. 2015. Study the static adsorption/desorption of formaldehyde on activated carbons. *International Forum on Energy, Environment Science and Materials (IFEESM 2015)*, p. 943-947. China: *Advances in Engineering Research*.
- Mak, S. M., Tey, B. T., Cheah, K. Y., Siew, W. L. and Tan, K. K. 2009. Porosity characteristics and pore developments of various particle sizes palm kernel shells activated carbon (PKSAC) and its potential application. *Adsorption* 15: 507-519.
- Mi, T., Chen, L., Xin, S. Z. and Yu, X. M. 2015. Activated carbon from the Chinese herbal medicine waste by  $H_3PO_4$  activation. *Journal of Nanomaterials* 2015: 1-9.
- Min, D. B. and J. M. Boff, J. M. 2002. Chemistry and reaction of singlet oxygen in foods. *Comprehensive Reviews in Food Science and Food Safety* 1: 58-72
- Muhammad, Choong, T. S. Y., Chuah, T. G., Yunus, R. and Yap, Y. H. T. 2010. Adsorption of  $\beta$ -carotene onto mesoporous carbon coated monolith in isopropyl alcohol and n-hexane solution: equilibrium and thermodynamic study. *Chemical Engineering Journal* 164: 178-182.
- Muhammad, Choong, T. S. Y. Chuah, T. G. Yunus, R. and Yap, Y. H. T. 2011. Desorption of  $\beta$ -carotene from mesoporous carbon coated monolith: Isotherm, kinetics and regeneration studies. *Chemical Engineering Journal* 173: 474-479.
- Rahman, M. M., Adil, M. and Yusof, A. M. 2012. Porosity development in activated carbon from palm kernel and coconut shell by chemical activation method. *Research Journal of Chemistry and Environment* 16(4): 189-191.
- Silva, S. M., Sampaio, K. A., Ceriani, R., Verhe, R., Stevens, C., Grey, W. D. and Meirelles, A. J. A. 2013. Adsorption of carotenes and phosphorus from palm oil onto acid activated bleaching earth: equilibrium, kinetics and thermodynamics. *Journal of Food Engineering* 118: 341-349.
- Ulfah, M., Raharjo, S., Hastuti, P. and Darmadji, P. 2016. The potential of palm kernel shells activated carbon as an adsorbent for  $\beta$ -carotene recovery from crude palm oil. *AIP Conference Proceedings* 1755: 130016-1-130016-5.
- Üner, O., Geçgel, Ü. and Bayrak, Y. 2015. Preparation and characterization of mesoporous activated carbons from waste watermelon rind by using the chemical activation method with zinc chloride. *Arabian Journal of Chemistry*. (In Press).
- Yusufu, M. I., Ariaahu, C. C. and Igbabul, B. D. 2012. Production and characterization of activated carbon from selected local raw materials. *African Journal of Pure and Applied Chemistry* 6(9): 123-131.
- Zeb, A. 2011. Effects of  $\beta$ -carotene on the thermal oxidation of fatty acids. *African Journal of Biotechnology* 10(68): 15346-15352.
- Zeb, A. and S. Mahmood. 2004. Carotenoids contents from various sources and their potential health applications. *Pakistan Journal of Nutrition* 3(3): 199-204.